Since all the cycles in the process must be opened, and since the number of streams in a decomposition is finite, such a procedure must terminate and lead to a nonredundant family.

*Theorem 4*: A family of decompositions contains at least $u$ decompositions, where $u$ is the number of units in the looped process system.

*Proof*: A process flow graph for a recycle system is a connected graph, that is, there exists a directed path from any vertex to any other vertex. Consider a decomposition $\{D_1\}$ where unit 1 has all its inputs torn. One application of the Replacement Rule would replace these inputs by the outputs of unit 1. Call this decomposition $\{D_2\}$. Once again, there exists a unit with all inputs torn. Call it unit 2. This process of replacement and renumbering of units can be continued for at least $u$ units. Therefore, there must be at least $u$ decompositions in any decomposition family.

*Manuscript received August 2 and accepted September 13, 1974.*

# Some Fundamental Aspects of Spray Drying

**Equations are proposed to predict the three-dimensional motion of droplets in a spray dryer, based on a knowledge of the characteristics of the atomizing device and of the gas flow patterns in the drying chamber. If the droplet size distribution produced by the atomizing device is known or can be assumed, the trajectories of the droplets can be calculated throughout the drying process and hence the evaporative capacity and thermal efficiency of the spray dryer can be predicted.**

**Experimental verification of this theoretical approach was obtained from a study of the drying of calcium lignosulfonate solutions of various concentrations in a 122-cm diam. × 183-cm high laboratory circular concurrent chamber with a conical bottom where the drying air was introduced tangentially near the top.**

**An experimental study of the effects of a number of operating variables on the capacity and the efficiency of the spray dryer was also carried out. These effects were interpreted in terms of the droplet trajectories obtained in each case.**

**S. KATTA and W. H. GAUVIN**

**Department of Chemical Engineering**
**McGill University**
**Montreal, Quebec, Canada**

## SCOPE

Among the many drying methods available, spray drying has gained a unique and important position in industrial applications where low particle temperatures and short residence times are specially advantageous, such as in the drying of foods, drugs, and temperature-sensitive materials in general. Prediction of droplet trajectories and residence times is essential for the sound design and efficient operation of spray dryers. Such knowledge can also be applied in the design of a number of other equipment involving the contacting of a dispersed phase of droplets or particles with a conveying gas, such as spray coolers, gas scrubbers and absorbers, cyclone evaporators, pneumatic transport reactors, and combustion devices involving fuel sprays. Many attempts were made in the past to predict droplet trajectories in spray dryers, but these were based on unrealistic or oversimplified models, which failed to take into account the many complex interdependencies between the transport phenomena occurring during the drying process and thus generally resulted in poor agreement between theoretical predictions and the actual performance of the system.

The objective of the present study was to predict the trajectories of droplets both in the nozzle zone (the region traversed by the rapidly-decelerating droplets between the exit of the atomizing device and the point at which they begin to be freely entrained by the drying gas) and in the free-entrainment zone (where the droplets are freely conveyed by the drying gas) of an experimental spray dryer, using solutions of calcium lignosulfonate (trade-mark LIGNOSOL) as the model material. Predictions of drop size distribution (DSD) and of the size of the largest droplet generated by the nozzle were also developed, as this knowledge is vital for the calculation of the trajectories. The three-dimensional equations of motion of the droplets, along with the equations for particulate heat transfer, for the mass transfer of water vapor and for the changes in the properties of the drying gas were solved numerically and simultaneously on a computer.

To test these theoretical predictions, the effect of a number of operating variables such as the temperature and flow rate of the drying gas, the position of the atomizing nozzle in the chamber, and the concentration of the feed on the evaporative capacity and the thermal efficiency of the spray-drying chamber have been studied experimentally. These experimental results were interpreted in terms of the droplet trajectories obtained under the various operating conditions used.

In an earlier paper, Gauvin et al. (1974) predicted droplet trajectories for the evaporation of water sprays in the same equipment as was used in the present study.

Good agreement was obtained between the theory and the experimental results. This prior investigation was extended to the spray drying of calcium lignosulfonate solutions in the study reported here, as the presence of dissolved solids significantly alters the process of evaporation from pure liquids.

## CONCLUSIONS AND SIGNIFICANCE

The study has clearly established that it is possible to calculate, on a completely theoretical basis, the momentum, heat, and mass transfer to droplets in both the nozzle zone and the free-entrainment zone of a spray-drying chamber, as above defined. It has also been shown that the prediction of the initial drop size distribution and of the largest droplet size can be made with reasonable accuracy solely on theoretical considerations.

Calculations of the droplet path in both zones are in reasonable agreement with the experimental observations. For two different sets of operating conditions, both carried out at the corresponding maximum evaporative capacity of the chamber, calculations showed that the largest droplet should become almost dry by the time it reached the wall of the chamber, while for a slightly larger feed rate or a slightly larger droplet, wet particles should hit the wall, in agreement with the experimental evidence, thus establishing the validity of the method of prediction.

The effects of the various operating parameters studied on the evaporative capacity and the thermal efficiency of the spray dryer were interpreted on the basis of the trajectories obtained. In general, capacity and efficiency will increase as the heat and mass transfer rates to droplets increase and as the droplet path becomes longer. In addition, efficiency is strongly affected by heat losses. Any operating variable which affects the above factors will correspondingly affect the spray-dryer capacity and efficiency.

The most significant of the effects studied is the influence exerted by the position of the atomizing nozzle. This effect was magnified because of the relatively small size of the chamber. It can be inferred from the work of Schowalter and Johnstone (1960) that when the nozzle is close to the roof of the chamber, the droplet enters the entrainment zone of its motion in a region of high vertical velocity due to the pronounced downward pitch of the flow and is rapidly conveyed towards the wall. On the other hand, when the nozzle is situated below the optimum position, although the smaller pitch of the flow in the lower part of the cone is favorable, the narrowing diameter of the chamber and the increased tangential velocity decrease the droplet's residence time. As the concentration of the feed is raised, the diameter of the largest droplet increases which in turn increases its initial momentum and the required drying time. This, by virtue of the mechanism discussed above, necessitates a progressively lower position of the nozzle for maximum performance.

A marked decrease in capacity with an increase in the concentration of the feed was observed. This is due to the fact that the average droplet size and, hence, the largest droplet size, increase with the feed concentration, as just explained. Finally, an optimum drying gas temperature for maximum capacity is shown to exist for each of the concentrations studied.

It is believed that the method of predicting the droplet size distribution and the computational approach employed in the present study can be extended to the spray drying of other solutions, providing that the particles of spray-dried product are not hollow. In the latter case, experimental information on the characteristics of the product must be obtained prior to the calculations.

---

### PREVIOUS WORK

Baltas and Gauvin (1969a, b) reviewed critically the work on transport phenomena in spray drying until 1967, while Masters (1972) presented a more general review of the whole field. Gauvin et al. (1974) covered the most recent published literature and reported their study on the prediction of droplet trajectories for water sprays in the nozzle zone and in the free-entrainment zone in a cylindrical concurrent spray drying chamber with a conical bottom in which the drying air was introduced tangentially near the top. The importance of the droplet trajectories and their effect on the capacity and efficiency were also discussed. This study was based on a more realistic model than any attempted in the past. Recent and some past studies pertinent to the present paper will now be discussed.

Dlouhy and Gauvin (1960a) studied the spray drying of calcium lignosulfonate solutions in a concurrent downflow spray dryer. Among the important observations reported were that no significant falling-rate period could be noticed and that up to a concentration of about 20%, calcium lignosulfonate solutions exhibited typical colloidal properties, while above that concentration a decrease in vapor pressure took place. They predicted accurately the drying time for the spray, employing a step-by-step method to follow the droplets of different sizes present in the spray. In a second paper (1960b), the same authors reported a study on the evaporation of water sprays and concluded that droplets below about 40 $\mu$m diameter evaporated at the same rate as single, stationary droplets evaporating in still air. However, it was pointed out by Bose (1963) that the relative motion between the droplets and the air stream cannot be neglected if this relative motion is of significant magnitude, as is generally the case for larger droplets.

The experimental study of Manning and Gauvin (1960) on heat and mass transfer rates to water sprays in the nozzle zone is of particular significance since they measured the droplet velocities near the nozzle and the temperature of the drying gas within the spray. Gluckert (1962) presented simplified equations for droplet trajectories, on the basis of which he proposed correlations for the design of spray dryers. His study was based on the assumption that droplets have the same velocity as that of the drying gas, which is not valid in view of the large sizes (30 $\mu$m to 200 $\mu$m) generally encountered in spray drying.

Baltas and Gauvin (1969b) proposed an accurate but complex stepwise procedure to follow the evaporation and drying of a sodium nitrate spray in the free-entrainment zone of a downward concurrent spray dryer. More recently, Janda (1973) developed a method to design spray dryers employing centrifugal disk atomizers on the basis of two-

dimensional trajectories of droplets in the dryer. His assumption, that the droplets follow the gas near the wall of the chamber, is not justified. Parti and Palancz (1974) presented a mathematical model for spray drying with a number of simplifying assumptions which make the model somewhat unrealistic. Finally, an extensive literature survey on all aspects of spray drying was presented by Mochida and Kinuta in 23 articles (1971-73).

The present study is reported in three sections, namely (1) drop size distribution, (2) trajectories of droplets, and (3) spray-drying efficiency and capacity.

## EXPERIMENT

### Equipment

For the present investigation, solutions of calcium lignosulfonate (trade-mark LIGNOSOL) of 5, 7.5, and 10% concentration by weight were used as feed. For each set of operating conditions, the maximum evaporative capacity of the chamber was determined according to the criterion that no incompletely dried particle should hit the walls of the chamber. This could be easily observed experimentally through the windows provided for that purpose since even slightly wet particles would stick to the glass. The maximum capacity (above which sticky particles would collect on the windows) was easily defined and quite reproducible. Although more demanding, this criterion was found to be experimentally preferable to its alternative, namely, that no wet particles should be present in the exit gas.

The equipment consisted briefly of a gas-heated furnace, followed by a blower, to provide the drying air; the spray-drying chamber, a concurrent downflow type with tangential air entry; a pneumatic nozzle assembly and a multicone-type cyclone collector. The chamber was constructed of 0.015-cm thick galvanized steel and consisted of a 1.22-m I.D. × 0.61-m high upper jacketed cylindrical section and a 1.22-m high lower conical section.

The hot air from the blower was introduced tangentially into a 5.08-cm wide annular jacket surrounding the cylindrical section and then distributed to the chamber through six slots (3.81-cm × 15.2-cm) cut in the inside wall at an angle of 45°. The metal was not cut out, but merely bent back along a 90-degree edge to produce a fairly tight spiral flow. The entire chamber and entering ducts were coated internally with a high-temperature aluminum paint and heavily insulated with 'Tartan' cement. Greater details were provided in the earlier paper (Gauvin et al., 1974).

An internal-mixing pneumatic nozzle (Spraying Systems Co. type 22-B, orifice diameter = 0.356 cm) was used exclusively. The pressure of the atomizing air was precisely controlled by a needle valve and its flow rate was measured by an orifice. The nozzle position could be adjusted at any desired level in the chamber. A schematic diagram of the spray dryer is given in Figure 1. A sketch of the above nozzle was given by Masters (1972).

### Procedure

The maximum capacity of the chamber at steady state, for given operating conditions, was determined by gradually increasing the feed rate until the particles of calcium lignosulfonate started to adhere to the observation windows, located in the conical section. As the chamber was flushed out after each set of runs, wet particles of solids adhering to the windows could easily be detected. Dry particles, on the other hand, did not adhere at all, but were carried out by the gas stream. All the temperatures, pressures, and flow rates were recorded when the maximum capacity was reached.

## DROP SIZE DISTRIBUTION

The important characteristics of a spray are the average droplet diameter, the droplet size distribution and the largest droplet size. These will now be discussed in turn. Nukiyama and Tanasawa (1938) presented the following empirical correlation to predict the average droplet size in the case of pneumatic atomization from an extensive experimental study:

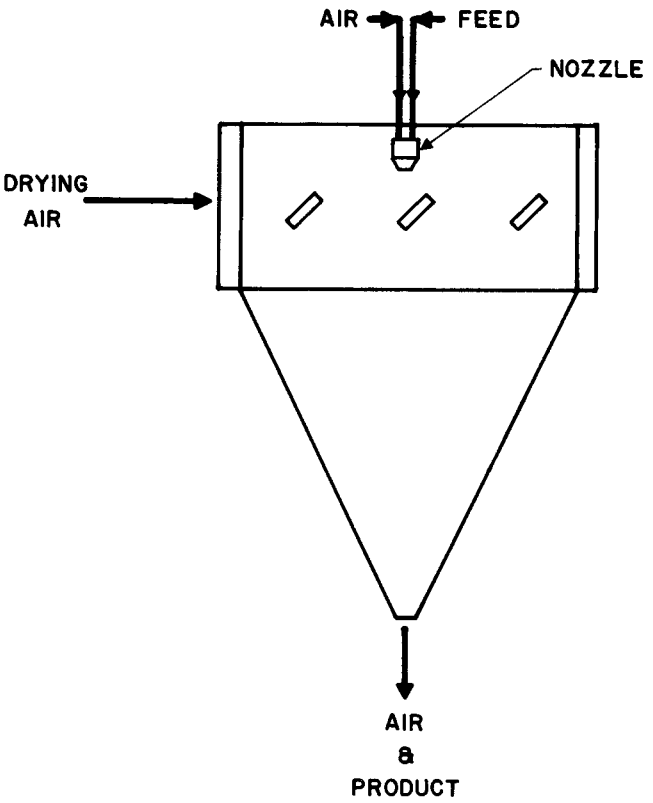


Fig. 1. Schematic diagram of spray dryer.

$$d_{vs} = \frac{585}{V_{\text{rel}}}\left(\frac{\sigma}{\rho}\right)^{0.5} + 597\left(\frac{\mu}{\sqrt{\sigma\rho}}\right)^{0.45}\left(\frac{1000\,Q_l}{Q_a}\right)^{1.5} \quad (1)$$

The above equation was verified by several experimenters. Nukiyama and Tanasawa presented a second empirical equation to express the size distribution as follows:

$$n_i/\Delta d = a\,d_i^2 \exp\,(-bd_i^q) \quad (2)$$

Lewis et al. (1948) showed that $q$ is a constant for a given nozzle over a wide range of operating conditions and must be determined experimentally.

Kim and Marshall (1971) proposed correlations for obtaining an average droplet size and size distribution from an experimental study, employing a novel technique of spraying a molten wax and melts of wax-polyethylene mixtures. It is not clear from the literature how these correlations compare with those of Nukiyama and Tanasawa.

The controlling influence of the largest droplet in many spray-drying operations is quite apparent. Mugele and Evans (1951) proposed a method which utilizes a special upper-limit function to obtain the size of the largest droplet. This method will be explained in detail later. Gwyn et al. (1965), from particle-size analysis by the count method, found that the largest observed size fell in the vicinity of the 0.9986 level within the cumulative distribution of the parent population.

The experimental data obtained on drop size distribution with water as the feed will now be treated in order to determine the characteristics of the atomizing nozzle used in this study. A plot of log $[n_i/(d_i^2\,\Delta d)]$ vs. $d_i^2$, as shown in Figure 2, yielded a straight line showing that the value of $q$ in Equation (2) is 2. Hence, the equation to represent the drop size distribution for the atomizing nozzle employed in this study is

$$n_i/\Delta d = ad_i^2 \exp\,(-bd_i^2) \quad (3)$$

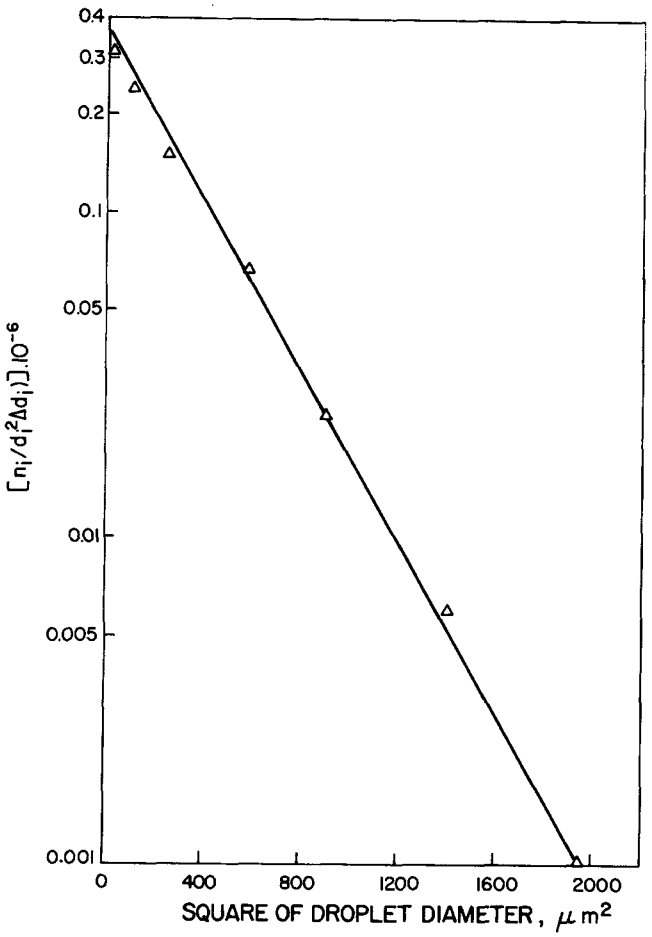


Fig. 2. Experimental drop size distribution for water.

where $a$ and $b$ are constants which depend upon the operating conditions. From a mathematical analysis, Nukiyama and Tanasawa obtained the following relations:

$$b = 2.25/d_{vs}^2 \tag{4}$$

$$a = 1.91\ b^3 V \tag{5}$$

where $V$ = total volume of the sample, cubic microns. The value of $d_{vs}$ obtained experimentally agreed reasonably well with that predicted from the Nukiyama-Tanasawa equation. Following the method of Mugele and Evans, the above DSD for water was treated to obtain the probable upper limit size, $d_m$. A value of $d_m$ is found that gives the best fit when $\log [d_i/(d_m - d_i)]$ is plotted against the cumulative number frequency on a probability grid, as shown in Figure 3, by a trial and error procedure. The experimental value of $d_m$, in this case, is in the range of 62 to 65 $\mu$m, which is in excellent agreement with that obtained by the above method.

For the calcium lignosulfonate solutions employed in the present study, Equation (1) was used to predict $d_{vs}$ and Equations (3), (4), and (5) were used to estimate the droplet size distribution. The size of the largest droplet was determined by the upper-limit analysis outlined above, and found to be 95 $\mu$m, as shown in Figure 4.

It should be mentioned that very recently Licht (1974) analyzed the data obtained by Kim and Marshall (1971) on pneumatic atomizers using the upper-limit function. He found that the maximum drop size would be close to 3.0 times the mass-median size. Kim and Marshall showed that the Sauter mean diameter would be equal to 0.83 times the mass-median diameter. However, the experimental work of Miyasaka (1959) indicates, from very scattered data, that the ratio of $d_m/d_{vs}$ varies from 1.8 to 3.0 depending on the operating conditions.

## TRAJECTORIES OF DROPLETS

Prediction of droplet trajectories requires the solution of a set of simultaneous equations to express (1) the three-dimensional motion of the droplets; (2) their instantaneous evaporation rate; (3) the three-dimensional flow pattern of the drying gas, and (4) the instantaneous properties of the latter. These will now be treated in turn.

The equation of motion of a droplet in centrifugal and gravitational fields can be expressed as

$$dV_f/dt = g + r\omega^2 + V_t V_r/r - C_D V_f^2 \rho_a A_p/2m + F_L/m \tag{6}$$

Resolving this equation in the three dimensions, the droplet velocities can be written as follows:

$$dV_t/dt = -V_t V_r/r - 3C_{D\rho a} V_f (V_t - V_{at})/4d_i\rho \tag{7}$$

$$dV_r/dt = V_t^2/r - 3C_{D\rho a} V_f (V_r - V_{ar})/4d_i\rho + F_L/m \tag{8}$$

$$dV_v/dt = g - 3C_{D\rho a} V_f (V_v - V_{av})/4d_i\rho \tag{9}$$

where $V_f$, the velocity of the droplet relative to the fluid, is given by

$$V_f^2 = (V_t - V_{at})^2 + (V_v - V_{av})^2 + (V_r - V_{ar})^2 \tag{10}$$

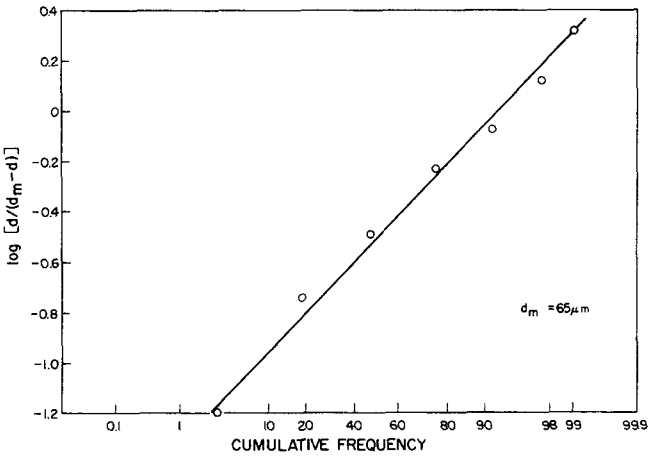


Fig. 3. Prediction of maximum droplet size for water.

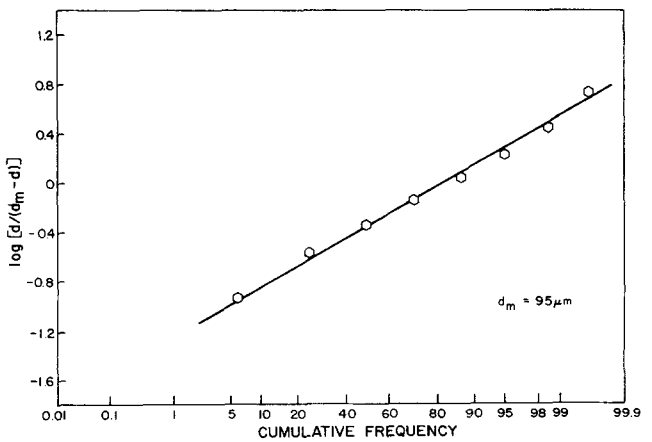


Fig. 4. Prediction of maximum droplet size for 10% calcium lignosulfonate solution.

The drag coefficient was evaluated by means of the equations proposed by Beard and Pruppacher (1969) for different ranges of $Re$, which are generally considered to be the most reliable of the equations available in the literature.

The shear lift force on the droplets was estimated from the following equation presented by Saffman (1965) for the motion of a sphere in an unbounded shear flow:

$$F_L = 20.25\rho_a d_i^2 (\nu_a/K)^{0.5} KV_f \qquad (11)$$

where $K$ is the curl of the fluid velocity, which can be shown to be equivalent to

$$K = 1.4\ V_{av}\ (r/r_5^2) \qquad (12)$$

when the axial jet velocities are estimated from the following equation (Pai, 1954):

$$V_{av} = V_c \cdot \exp\ [-0.692\ (r/r_5^2)] \qquad (13)$$

The shear lift force was assumed to be negligible when the droplet $Re$ was greater than one. The lift force due to spin was estimated to be negligible in the present study. A fuller treatment of this section is given in the paper by Gauvin et al. (1974).

#### Droplet Evaporation Rate

The droplet evaporation rate is given by

$$dm_i/dt_i = \pi h d_i^2 n_i\ (t_a - t_s)/\lambda \qquad (14)$$

where the heat transfer coefficient $h$ was determined from the following correlation proposed by Ranz and Marshall (1952):

$$Nu = 2.0 + 0.6\ (Re)^{0.5}\ (Pr)^{0.33} \qquad (15)$$

The instantaneous diameter of any droplet was determined from the following equation:

$$d_i = d_{in}\ [\rho_{in}/c_i \cdot \rho_i]^{0.33} \qquad (16)$$

where the subscripts $i$ and $in$ represent the instantaneous values and the initial values, respectively, of the same droplet class.

The temperature of the droplet at any particular concentration was determined from the psychrometric chart shown in Figure 5 which was obtained by Dlouhy and Gauvin (1960).

#### Gas Flow Patterns

Among the main difficulties encountered in the design of spray dryers is the lack of accurate information on the flow patterns prevailing in the spray-drying chamber. In the present study, the flow in the chamber was very complex and due to lack of information on the interaction of a vortex flow on a jet, the flow was assumed as a superposition of the jet of atomizing fluid and the surrounding centrifugal field of the drying air.

The centerline velocities of the jet were computed from the equations of Gal (1970) given below:

$$V_c/V_o = 6.5/\bar{x} \qquad (17)$$

where

$$\bar{x} = (\rho_\alpha/\rho_o)^{0.5}\ (x/D_o) \qquad (18)$$

The radial distribution of axial velocities was assumed to follow Equation (13) given earlier. The velocity half-radius was chosen to follow the following equation after examining the results reported in the literature:

$$r_5 = 0.09\ x \qquad (19)$$

The radial velocities reported by Albertson et al. (1950) were used in the computations.

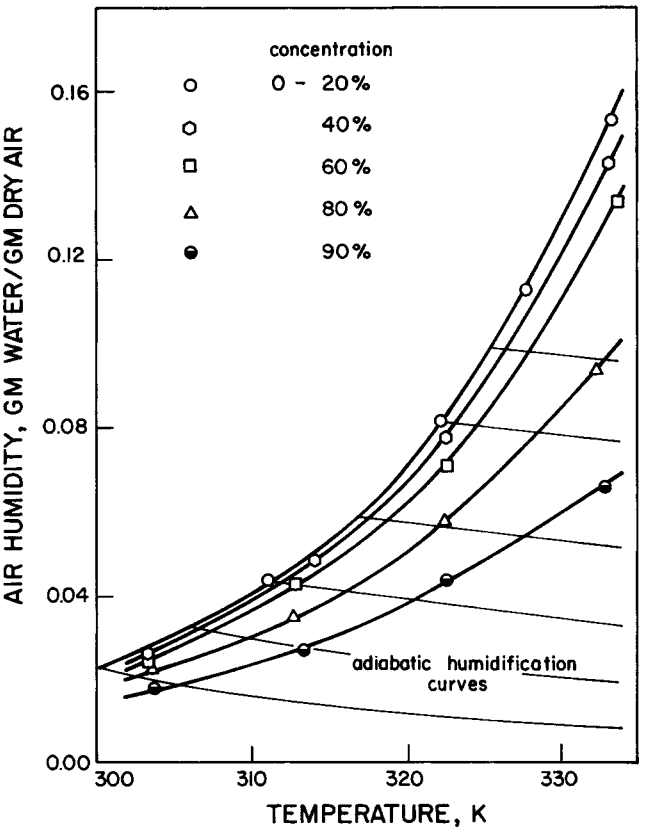


Fig. 5. Saturation humidities of calcium lignosulfonate solutions.

In the entrainment zone, the measured tangential air velocities, as reported by Gauvin et al. (1974), show that the vortex flow consists of a central zone and an annular zone near the wall, in which $V_{at}$ varies according to the two following equations, respectively:

$$V_{at} = C_1 r \qquad (20)$$

$$V_{at} = C_2\ (R - r) \qquad (21)$$

where $C_1$ is a function of the axial distance from the nozzle and $C_2$ remains constant. Vertical velocities were calculated on the assumption that they remained constant along a horizontal plane.

#### Properties of Drying Gas

The temperature of air $t_a$ at a position $z$ in the nozzle zone was estimated from an energy balance in this zone which yields the following equation:

$$(t_a - t_w) = \{M_e(0.24 + 0.45\,H_1)\,(t_{a1} - t_w) + W_L(t_f - t_w) - [(M_e + M_o)\,(H_z - H_1)\lambda_w]\}/[(M_e + M_o)\,(0.24 + 0.45\,H_z)] \qquad (22)$$

The heat losses were neglected in the above equation. $H_z$ was estimated from the equation

$$H_z = E_z/(M_e + M_o) + H_1 \qquad (23)$$

It was assumed that no radial temperature gradients existed. This seems reasonable in view of the fact that mixing of the drying gas with the atomizing fluid was quite intense. Further, the complexity of the flow prevents any reasonable estimation of the temperature gradients present in the dryer. The rate of entrainment at any section of the jet was estimated from the following equation proposed by Davies (1972):

$$M_e = M_o\ [0.23\ (x/D_o) - 1] \qquad (24)$$

In the free-entrainment zone, the temperature of the air at any position $z$ in the path of the droplets was obtained from an overall energy balance which yielded the following equation:

$$W_G(t_1 - t_w)\, C_{s1} + W_L(t_f - t_w) = W_G(t_a - t_w)C_{sz} + E_z\lambda_w + q_{lz} \quad (25)$$

Heat losses were assumed to be proportional to the evaporation which had occurred up to point $z$. The viscosity and thermal conductivity of air were determined from the equations reported by Hilsenrath et al. (1955).

#### Method of Calculations

As mentioned earlier, the experimental criterion used in this work for determining the maximum capacity of the spray drying chamber for a given set of operating conditions was based on the requirement that no wet droplet should impinge on the wall. Whether the theoretical model agrees with the experimental observation for a given set of operating conditions can now be ascertained from a numerical solution of the equations of motion for the various classes of droplets simultaneously with the other equations developed earlier.

The computations were carried out on an IBM 360/75 computer. Since all the equations have to be solved simultaneously, a variable time increment depending on the size of the droplet was chosen so that all the droplets would advance to the same plane perpendicular to the axis of the chamber. In other words, at any instant, the same distance step was used for all classes of droplets, which was fixed by the velocity of the smallest droplet whose trajectory was being computed. In order to prevent the computations from becoming excessive, the droplets of three smaller sizes were assumed to follow the gas. This is justified in view of the experimental evidence of Dlouhy and Gauvin (1960b). The largest time increment used was $10^{-4}$ second initially and $10^{-3}$ second for most of the calculations.

## RESULTS

For the purpose of illustration, the results of calculations carried out for a specific set of operating conditions are presented here. The operating conditions for this experimental run were as given below:

| | |
|---|---|
| Mass flow rate of drying air, $W_G$ | = 354 kg/hr. |
| Temperature of inlet drying air, $t_1$ | = 458 K |
| Humidity of inlet drying air, $H_1$ | = 0.0356 |
| Feed temperature, $t_f$ | = 284 K |
| Feed concentration by wt. | = 10% |
| Mass flow rate of atomizing air, $W_A$ | = 27 kg/hr. |
| Nozzle position below roof | = 31.43 cm |
| Heat losses | = 1764 J/s |

The maximum evaporative capacity, under these experimental conditions, was experimentally determined to be 4.32 kg/hr. of water.

The initial conditions selected for the calculations corresponded to a plane located at 3.8 cm from the nozzle exit, at which position Manning and Gauvin (1960) measured velocities of droplets issuing from an identical nozzle. Since the relative locations of the droplets of different sizes were unknown, it was assumed that they were distributed evenly according to the size so that the largest size was at the edge of the spray and the smallest at a distance of one-eighth of the radius of the spray from its centerline. The temperature of the air within the spray was estimated from the rate of entrainment of surrounding gas into the jet. The droplet size distribution for these calculations was given earlier.

In the nozzle zone which extended a distance of about 76 cm below the nozzle, most of the evaporation and hence most of the change in air temperature took place. The temperature of drying air and the solid concentration of 80 and 95 $\mu$m droplets as a function of the axial distance and time, respectively, are shown in Figure 6. The effect of the lift force is also shown in the same figure. The change in the diameter of three classes of droplets with time is shown in Figure 7. It can easily be seen that a small increase in diameter requires an appreciably longer residence time for complete drying.

The calculations on the largest droplet indicated that it reached about 97% concentration when it hit the wall of the chamber. This is in good agreement with the experimental observation. The axial, tangential, and radial velocity components of this droplet are shown in Figure 8. The decrease of $V_v$ and $V_r$ of the droplet in the nozzle zone is

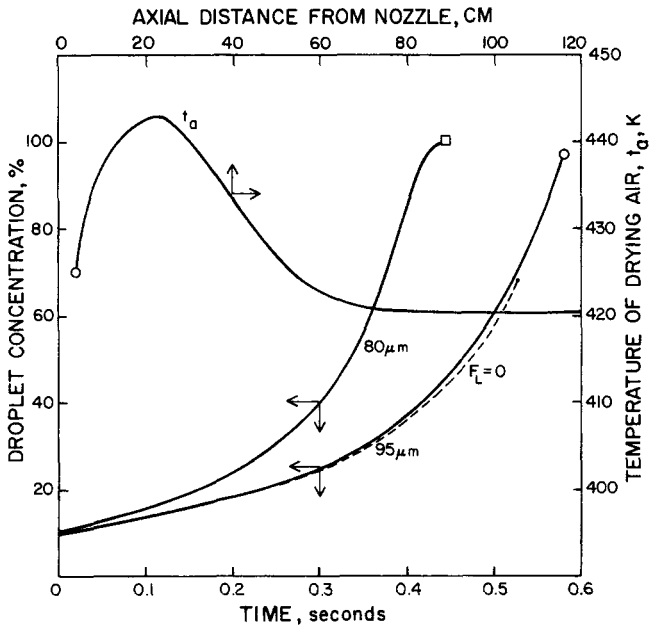


Fig. 6. Variation of droplet concentration and temperature of drying air.

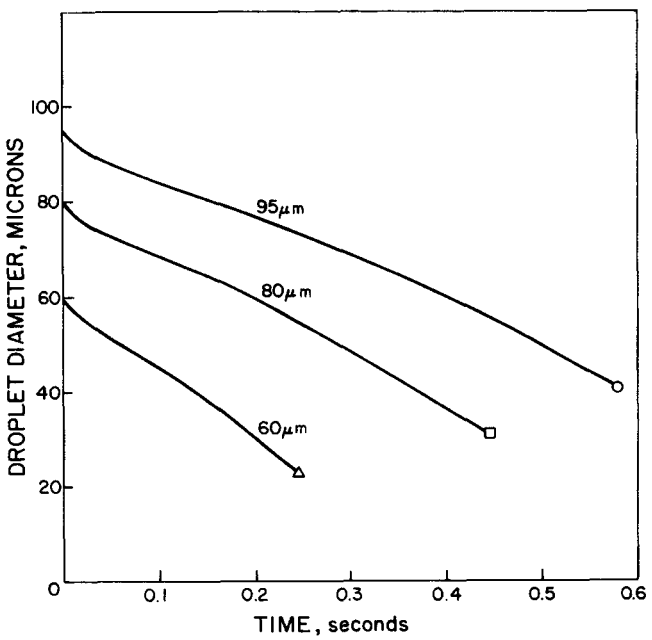


Fig. 7. Variation of droplet diameter with time.

due to the rapid deceleration of the droplet. The increase in $V_v$ in the latter part of the trajectory and also in $V_t$ is due to the converging flow field in the conical section of the chamber. The decrease in $V_t$ near the wall is due to the presence of an annular region where the gas tangential velocity decreases steeply towards the wall. The radial component, however, remains constant in the free-entrainment zone.

The axial and radial positions of droplets of two sizes as a function of time are shown in Figure 9. The change in angular position of 95 and 80 $\mu$m droplets with time is shown in Figure 10. A substantial difference between the two sizes existed in the final angular position.

## SPRAY DRYING CAPACITY AND EFFICIENCY

A study of the effects of a number of operating parameters such as the temperature of the feed, the flow rate, and the temperature of the drying gas, the pressure of the atomizing air and the nozzle depth on the capacity and thermal efficiency of a spray-drying chamber when water was the feed, was presented in an earlier paper (Gauvin et al., 1974). In the present study, the effects of the feed concentration, of the temperature of the drying gas and of the nozzle depth on the capacity and efficiency, where calcium lignosulfonate solutions were the feed, have been studied in detail.

The efficiency in the present study was defined as the ratio of heat used in vaporization to the total heat available and can be shown to be equivalent to the following expression:

$$\eta = W_w\lambda/[W_G\,(t_1 - t_w)C_{s1} + W_L(t_f - t_w)] \quad (26)$$

It is believed that this definition, if generally adopted by workers in the field, would facilitate comparison of chamber performance.

### Effect of Nozzle Position*

The effect of nozzle position on the capacity and efficiency of the spray dryer for different flow rates of drying gas (but at constant inlet temperature of ~ 420 K), in the case of 10% calcium lignosulfonate solution, is shown in Figure 11. The dramatic effect of the nozzle position on both capacity and efficiency and the existence of an optimum position is clearly shown in this figure. Further, this optimum position is independent of the flow rate of the drying gas. This is to be expected in view of the finding of Schowalter and Johnstone (1960) that the flow pattern of swirling flow is not affected by the volumetric flow rate. An explanation for the effect of the nozzle position has already been provided in the conclusions. At maximum capacity, the efficiency is also maximum; but at the optimum nozzle depth, the maximal values in both capacity and efficiency do not occur at the same flow rate. The same trends were observed for other solution concentrations.

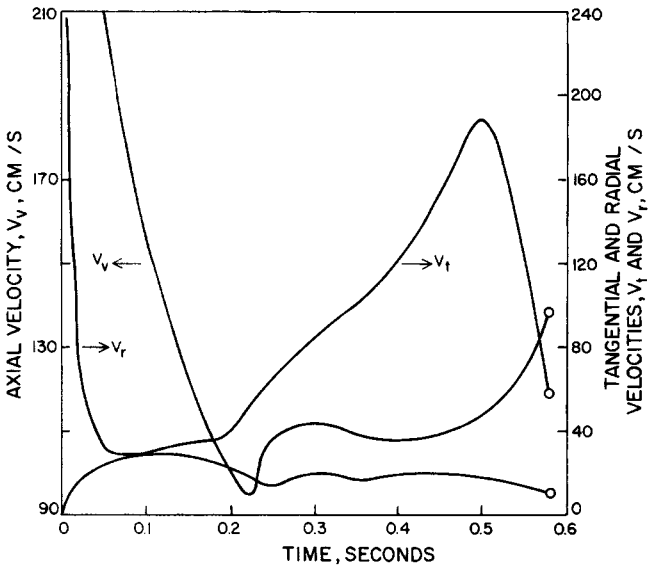


Fig. 8. Axial, tangential, and radial components of droplet velocity as a function of time.

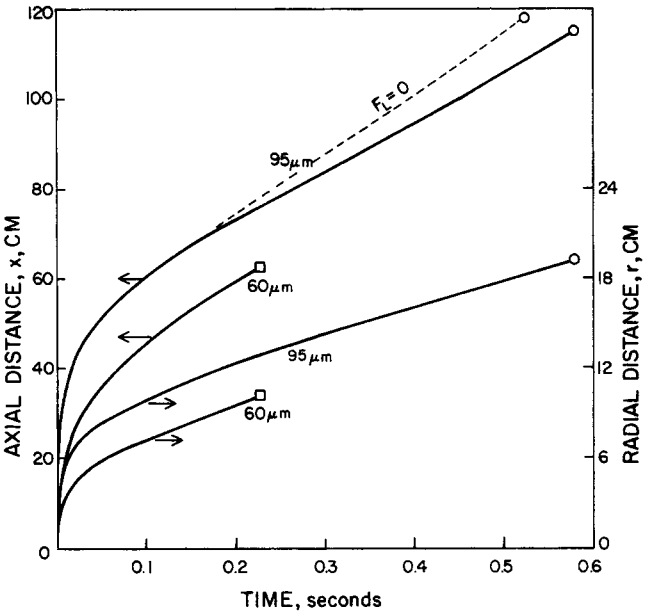


Fig. 9. Variation of droplet position with time.

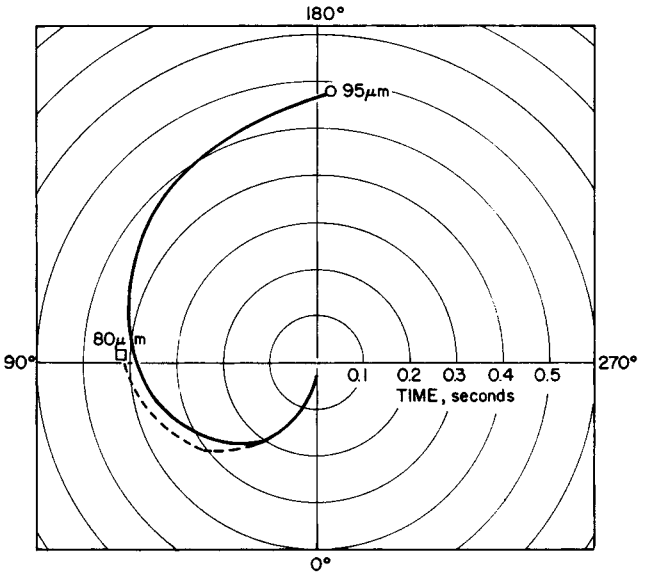


Fig. 10. Variation of angular position of droplet with time.

### Effect of Drying Gas Temperature

The effect of the temperature of the drying gas was investigated with the nozzle depth and gas mass flow rate constant at their optimum values for the different concentrations used. As the inlet gas temperature increases, its

* Detailed tables of results have been deposited as Document No. 02532 with the National Auxiliary Publications Service (NAPS), c/o Microfiche Publications, 305 E. 46th Street, New York, N.Y. 10017, and may be obtained for $1.50 for microfiche or $2.00 for photocopies.

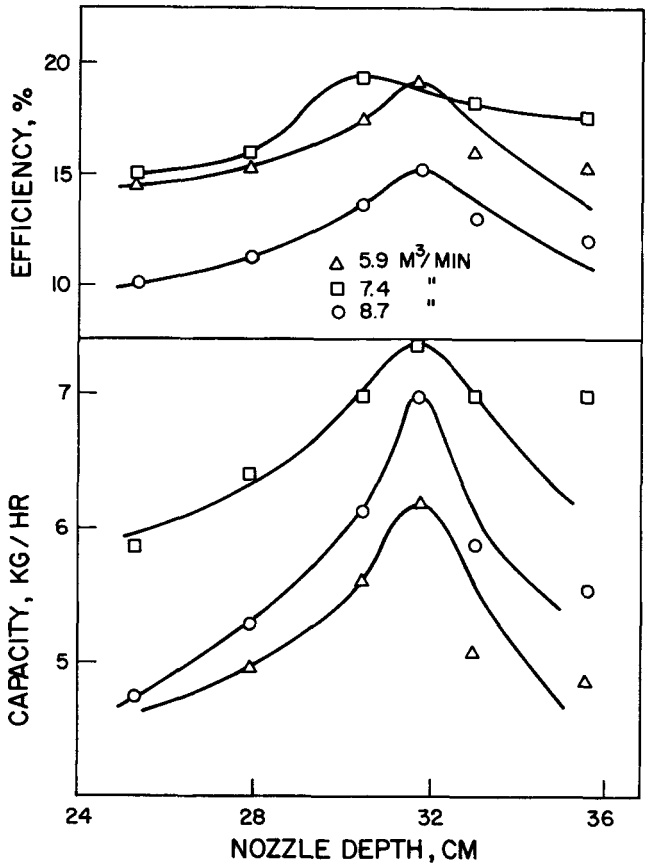


Fig. 11. Effect of nozzle position on evaporative capacity and efficiency for different flow rates of drying air (constant temperature of 490 K) for 10% solution.

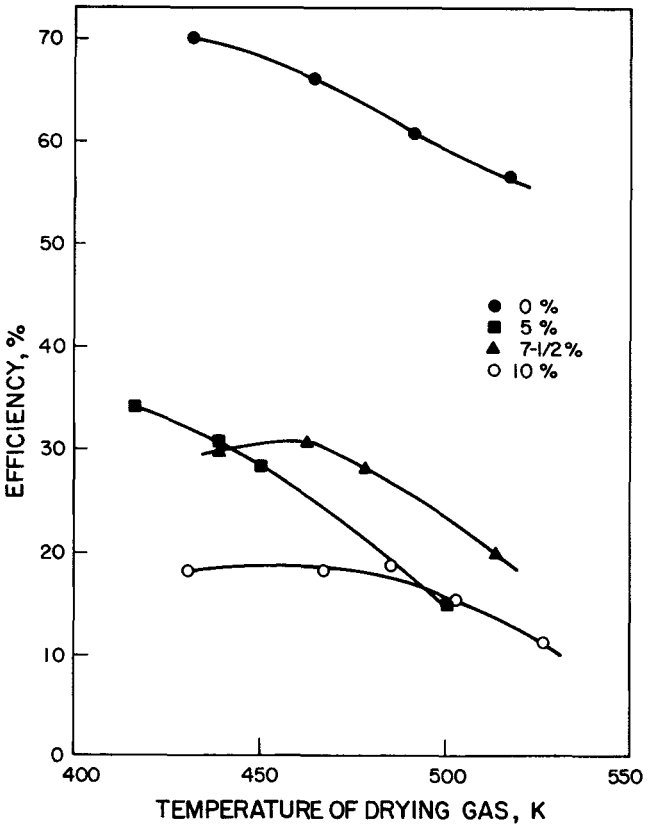


Fig. 13. Effect of temperature of drying air on efficiency for different concentrations of calcium lignosulfonate solutions at optimum nozzle position and volumetric flow rate.

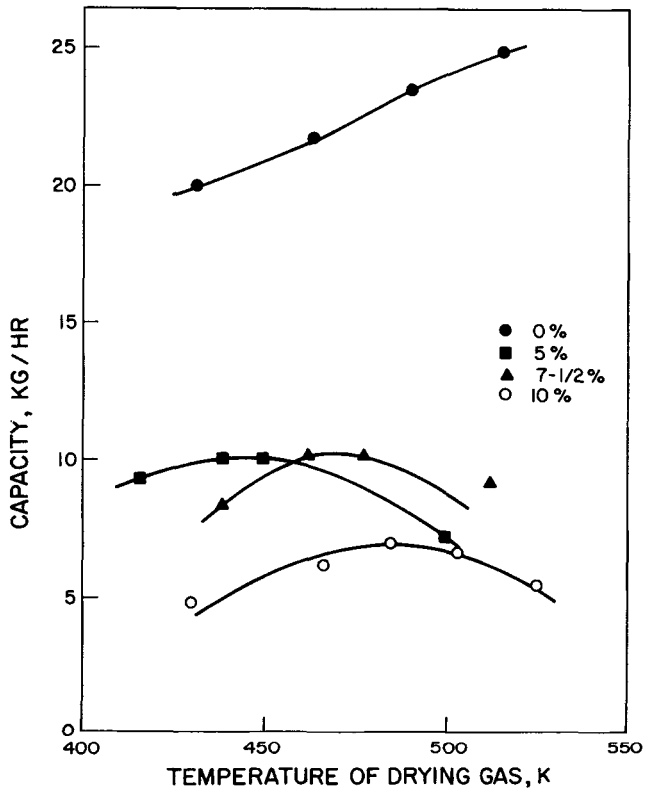


Fig. 12. Effect of temperature of drying air on evaporative capacity for different concentrations of calcium lignosulfonate solutions at optimum nozzle position and volumetric flow rates.

*volumetric* flow rate of course increases proportionately. Figures 12 and 13 summarize the effects on the capacity and the efficiency of the chamber.

In the case of calcium lignosulfonate solutions, the capacity first increases and then decreases sharply, demonstrating the existence of an optimum gas temperature for all the concentrations studied. As the inlet air temperature increases, both the heat transfer to the droplets and the latter's velocity increase. The former effect predominates until the optimum temperature is reached while the latter becomes the controlling factor beyond this temperature due to the shorter droplet path.

In the case of water as feed, the capacity of the chamber is much larger, primarily because the water droplets ($d_{vs}$ = 26 $\mu$m, $d_m$ = 65 $\mu$m) are much smaller than the droplets of calcium lignosulfonate solution ($d_{vs}$ = 50 $\mu$m, $d_m$ = 95 $\mu$m), and also because there is no diffusional resistance due to drying. The chamber capacity appears to increase steadily with the temperature, but will eventually level off and/or decrease at still higher gas temperatures.

The efficiency decreases with increase in the drying gas temperature due to poorer utilization of heat contained in the inlet drying gas and to the higher heat losses.

### Effect of Feed Concentration

The effect of the feed concentration on the capacity and the efficiency of the chamber, and also on the optimum nozzle depth and on the product yield, is shown in Figures 14 and 15. The drying gas temperature and flow rate were maintained constant in this series of runs. The dramatic decrease of the capacity with an increase in concentration can be explained as due to the increase in $d_{vs}$ and hence the size of the largest droplet, and also due to the slower rate of drying. The efficiencies of various runs were plotted

against concentration in the same figure. The curve closely follows that of capacity vs. concentration because the only variable in the expression for efficiency is the rate of evaporation of water.

Of even greater importance, from a practical point of view, is the yield of dried powder per unit time. As shown in Figure 15, the product yield increases with the concentration. Additional observations, which have not been reported here, indicate an optimum at a concentration of 15%.

The remarkable effect of the solution concentration on the optimum nozzle depth is shown in Figure 15.

## GENERAL COMMENTS

From a practical point of view, it must be admitted that the experimental part of this work suffered from two major weaknesses. The first is that the entrance arrangement for the drying air was poorly designed. By cutting the entrance slots at a 45° angle, the spiral of drying air was flung sharply downward towards the conical section. As a result, the upper section of the chamber was made largely ineffective from the point of view of droplet evaporation. As a consequence, the overall evaporative capacity of the chamber was unduly low, and the contribution of the nozzle zone to the total evaporation unduly high. It also exaggerated the importance of the nozzle position. The latter result may not have been entirely bad, however, since it certainly emphasized—more than any other observed effect—the importance of the droplet trajectory in the evaporation/drying process.

The second weakness is the paucity of experimental information on the flow pattern of the drying air and on its three-dimensional velocity distribution. The measured tangential air velocities reported by Gauvin et al. (1974) were not sufficient to provide the detailed information required, thus necessitating a number of assumptions, as explained in the pertinent section of the analysis. That these assumptions were reasonable seems to be shown from the good agreement between analytical and experimental findings. To remove any uncertainty, however, a detailed study of gas flow patterns, velocity distribution, and turbulence characteristics in a chamber identical to that used in the present work is currently under way in this laboratory.

One remaining point should be mentioned. In all the runs reported here, it was ascertained that the product consisted of dense, roughly spherical particles only. Data from runs yielding hollow spheres were discarded, as they invariably resulted in inordinately low chamber capacities. It is probable that hollow particles could also be handled by the technique outlined in this paper, providing enough information is available on the size, size distribution, and apparent density of the product.

Finally, it appears reasonable to conclude that the computational approach used in this study should hold equally well in the case of industrial-size spray-drying chambers, as well as in the case of other feed solutions.

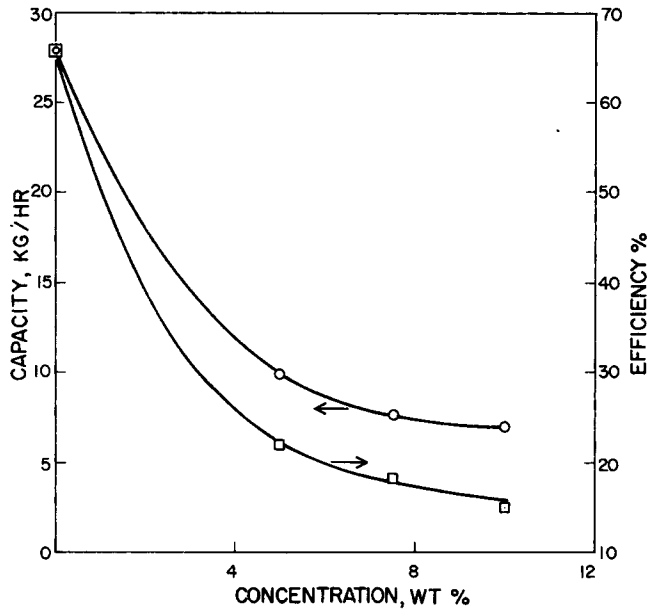


Fig. 14. Effect of concentration of calcium lignosulfonate solutions on evaporative capacity.

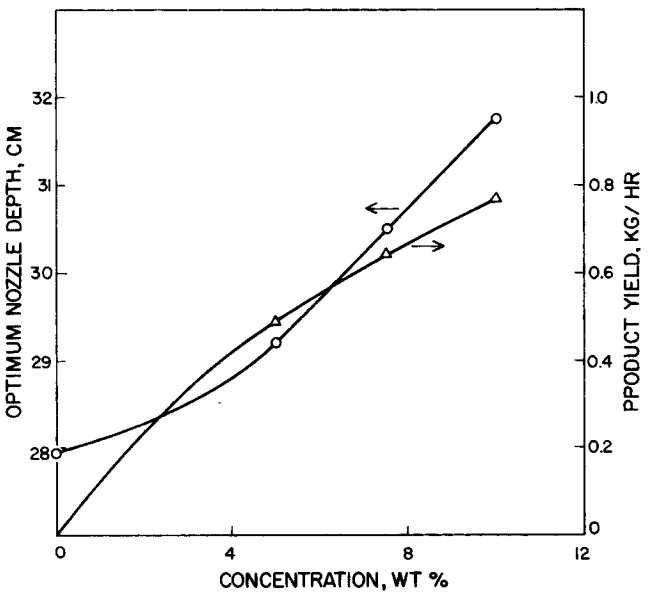


Fig. 15. Effect of concentration of calcium lignosulfonate solutions on optimum nozzle position and product yield.

## ACKNOWLEDGMENTS

This study is based on the experimental data of D. B. Lyons (M.Eng. thesis, McGill University, 1951) and on additional data of F. H. Knelman (M.Eng. thesis, McGill University, 1950). Financial assistance from the National Research Council of Canada is gratefully acknowledged.

## NOTATION

$a$, $b$ = parameters in Equation (2)
$C_1$, $C_2$ = constants
$A_p$ = projected area of droplet on a plane normal to mean flow, $m^2$
$C$ = droplet concentration, %
$C_D$ = drag coefficient
$C_p$ = heat capacity, J/kg·K
$C_{s1}$, $C_{s2}$ = heat capacity of inlet and outlet humid air, J/kg·K
$d_m$ = diameter of largest droplet, $\mu$m
$d_i$ = diameter of each class of droplets, $\mu$m
$D_o$ = diameter of nozzle, cm
$d_{vs}$ = mean Sauter diameter, $\Sigma n_i d_i^3/\Sigma n_i d_i^2$, $\mu$m
$E$ = rate of evaporation, kg/hr
$F_L$ = lift force, N
$g$ = acceleration due to gravity, $m/s^2$
$h$ = heat transfer coefficient, $J/m^2 \cdot s \cdot K$

$H_1$, $H_2$ = absolute humidities of entering and leaving air, respectively, gm of water vapor/gm of dry air
$k_a$ = thermal conductivity of air, J/m·s·K
$K$ = curl of fluid velocity, $s^{-1}$
$m$ = mass of droplet, kg
$M_e$ = mass flow rate of entrainment, kg/hr.
$M_o$ = mass flow rate of atomizing air, kg/hr.
$n_i$ = number of each class of droplets
$q$ = rate of heat transfer to droplets, J/s; constant in Equation (2)
$q_L$ = rate of heat losses from spray chamber, J/s
$Q_l$ = volumetric flow rate of liquid, $m^3$/hr.
$Q_a$ = volumetric flow rate of atomizing air, $m^3$/hr.
$r$ = radial position of droplet, cm
$R$ = radius of chamber at any height, cm
$r_5$ = velocity half-radius, cm (the radial distance where the centerline velocity becomes half)
$t$ = time, s
$t_a$ = temperature of drying air, K
$t_f$ = feed temperature, K
$t_d$ = datum temperature, K
$t_w$ = wet bulb temperature of drying air, K
$t_s$ = droplet temperature, K
$V$ = volume of feed sample, $\mu m^3$
$V_{at}$, $V_{ar}$, $V_{av}$ = absolute values of tangential, radial and axial velocities of air, respectively, m/s
$V_c$ = velocity of air on the centerline of atomizing jet, m/s
$V_f$ = resultant velocity of droplet relative to fluid, m/s
$V_o$ = velocity of air at nozzle exit, m/s
$V_t$, $V_r$, $V_v$ = absolute values of tangential, radial and axial velocities of droplet, respectively, m/s
$V_{rel}$ = relative velocity between the air stream and the liquid stream, m/s
$W_A$ = atomizing air flow rate, kg/hr
$W_G$ = flow rate of drying air; (free air, measured at 294 K and one atmosphere), kg of drying air/hr.
$W_L$ = flow rate of feed, kg/hr.
$W_w$ = chamber capacity, in kg of water evaporated/hr.
$\bar{x}$ = dimensionless distance, defined by Equation (18)
$x$ = vertical distance from nozzle, cm
$z$ = position along droplet path

### Greek Letters

$\Delta$ = increment
$\Delta d$ = the spread of the droplet size distribution
$\eta$ = drying thermal efficiency, defined by Equation (26)
$\theta$ = angular position of droplet, radians
$\lambda_d$ = latent heat of vaporization at $t_d$, J/kg
$\lambda_w$ = latent heat of vaporization at $t_w$, J/kg
$\mu_a$ = viscosity of air, N·s/$m^2$
$\mu$ = viscosity of liquid, poises
$\nu_a$ = kinematic viscosity of air, $m^2$/s
$\rho_a$ = density of air, kg/$m^3$
$\rho_\alpha$ = density of the surroundings of the jet, kg/$m^3$
$\rho$ = density of droplet, kg/$m^3$
$\sigma$ = surface tension of liquid, dynes/cm
$\omega$ = angular velocity of droplet, rad/s

### Dimensionless Groups

$Nu$ = Nusselt number, $hd_i/k_a$
$Pr$ = Prandtl number, $c_p\mu_a/k_a$
$Re$ = Reynolds number, $d_iV_f\rho_a/\mu_a$

### Subscripts

1 = at the inlet conditions of spray dryer
2 = at the outlet conditions of spray dryer
$a$ = of drying air
$d$ = at datum temperature
$in$ = at initial conditions
$o$ = at nozzle exit
$x$ = at a vertical distance $x$ below the nozzle
$w$ = at wet bulb temperature of the air
$z$ = at a position $z$ along the droplet path

### LITERATURE CITED


Albertson, M. L., Y. B. Dai, R. A. Jenson, and H. Rouse, "Diffusion of Submerged Jets," *ASCE Trans.*, **115**, 639 (1950).

Baltas, L., and W. H. Gauvin, "Performance Predictions for a Concurrent Spray Dryer," *AIChE J.*, **15**, 764 (1969a).

———., "Transport Characteristics of a Concurrent Spray Dryer," *ibid.*, 772 (1969b).

Bose, A. K., "Evaporation Rates in Spray Drying," M.A.Sc. thesis, Univ. Waterloo, Ontario, Canada (1963).

Beard, K. V., and H. R. Pruppacher, "A Determination of the Terminal Velocity and Drag of Small Water Drops by Means of a Wind Tunnel," *J. Atm. Sci.*, **26**, 1066 (1969).

Davies, J. T., *Turbulence Phenomena*, pp. 98, 99, Academic Press, New York (1972).

Dlouhy, J., and W. H. Gauvin, "Evaporation Rates in Spray Drying," *Can. J. Chem. Eng.*, **38**, 113 (1960a).

———., "Heat and Mass Transfer in Spray Drying," *AIChE J.*, **6**, 29 (1960b).

Gal, G., "Self-Preservation in Fully Expanded Turbulent Coflowing Jets," *AIAA J.*, **8**, 814 (1970).

Gauvin, W. H., S. Katta, and F. H. Knelman, "Drop Trajectory Predictions and Their Importance in the Design of Spray Dryers," *Intern. J. Multi-Phase Flow* (1974, in press).

Gluckert, F. A., "A Theoretical Correlation of Spray Dryer Performance," *AIChE J.*, **8**, 460 (1962).

Gwyn, J. E., E. J. Crosby, and W. R. Marshall, Jr., "Bias in Particle-Size Analysis by the Count Method," *Ind. Eng. Chem. Fundamentals*, **4**, 204 (1965).

Hilsenrath, J., C. W. Beckett, W. S. Benedict, L. Fano, H. J. Hoge, J. F. Masi, R. L. Nuttal, Y. S. Touloukian, and H. W. Woolley, "Tables of Thermal Properties of Gases," Nat. Bur. Standards Circ. No. 564 (1955).

Janda, F., "Calculation of the Dimension of Disc Spray Dryers with Intensive Circulation of the Drying Medium," *Intern. Chem. Eng.*, **13**, 649 (1973).

Kim, K. Y., and W. R. Marshall, Jr., "Drop Size Distributions from Pneumatic Atomizers," *AIChE J.*, **17**, 575 (1971).

Lewis, H. C., D. G. Edwards, M. J. Goglia, R. I. Rice, and L. W. Smith, "Atomization of Liquids in High Velocity Gas Streams," *Ind. Eng. Chem.*, **40**, 67 (1948).

Licht, W., "Maximum Drop Size Produced by Pneumatic Atomization," *AIChE J.*, **20**, 595 (1974).

Manning, W. P., and W. H. Gauvin, "Heat and Mass Transfer to Decelerating Finely Atomized Sprays," *ibid.*, **6**, 184 (1960).

Masters, K., *Spray Drying*, Leonard Hill Books, London, England (1972).

Miyasaka, Y., *Kikaigakkai Ronbunshu (J. Mech. Eng. Japan)*, **15**, (51), pp. 34-38 (1959).

Mochida, T., and Y. Kinuta, "Spray Drying," *Jap. J. Chem. Eng.* (1971-1973).

Mugele, R. A., and H. D. Evans, "Droplet Size Distribution in Sprays," *Ind. Eng. Chem.*, **43**, 1317 (1951).

Nukiyama, S., and Y. Tanasawa, "An Experiment on the Atomization of Liquid," *Trans. Soc. Mech. Engrs. (Japan)*, **4**, 86, 138 (1938); **5**, 63, 68 (1939); II-7 and II-8 (1940).

Pai, S., *Fluid Dynamics of Jets*, Van Nostrand, New York (1954).

Parti, M., and B. Palancz, "Mathematical Model for Spray Drying," *Chem. Eng. Sci.*, **29**, 355 (1974).

Ranz, W. E., and W. R. Marshall, Jr., "Evaporation from Drops, Part I," *Chem. Eng. Progr.*, **48**, 141 (1952).

———., *ibid.*, Part II, *ibid.*, **48**, 173 (1952).

Saffman, P. G., "The Lift on a Small Sphere in a Slow Shear Flow," *J. Fluid Mech.*, **22**, 385 (1965).

Schowalter, W. R., and H. F. Johnstone, "Characteristics of the Mean Flow Patterns and Structure of Turbulence in Spiral Gas Streams," *AIChE J.*, **6**, 648 (1960).



*Manuscript received August 26, 1974; revision received and accepted October 23, 1974.*